ACS OMEGA

http://pubs.acs.org/journal/acsodf

Article

Model Emulsions Stabilized with Nonionic Surfactants: Structure and Rheology Across Catastrophic Phase Inversion

Jie Jiang, Zi Wang, Chuangye Wang, Lina Shi, Jian Hou, and Longli Zhang*

Cite This: *ACS Omega* 2022, 7, 44012−44020

Read Online

ACCESS | Metrics & More | Article Recommendations | Supporting Information

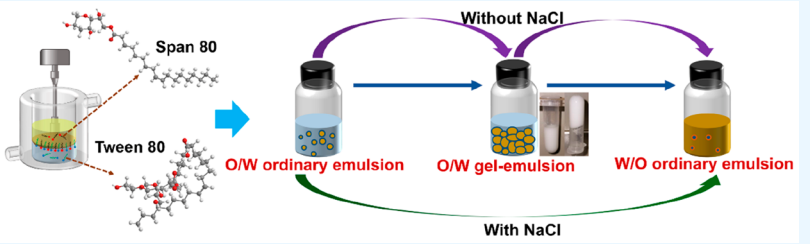

ABSTRACT: The catastrophic phase inversion process of model emulsions (water/Span 80-Tween 80/heptane) from oil-in-water to water-in-oil emulsion was investigated. During this process, the phase inversion of the emulsion was monitored through Fourier transform infrared spectroscopy (FT-IR). In emulsions without NaCl, oil-in-water gel emulsions are formed prior to phase inversion. As the HLB value increases, the oil volume fraction required for phase inversion becomes higher. Polydisperse distribution of the gel emulsion is observed from microscope optical images. The Turbiscan Lab stability analyzer indicates that O/W gel emulsions before the phase inversion has good stability at 50 °C. Rheological measurements reveal that emulsions exhibit non-Newtonian behavior. The viscosity of the gel emulsions increases significantly prior to phase inversion. As the oil volume fraction increases, the storage modulus and loss modulus of the gel emulsion increase to a maximum, at which catastrophic phase inversion occurs. In emulsions with NaCl, there is no oil-in-water gel emulsion formed before phase inversion. The physicochemical properties of the emulsion play a crucial role in whether gel emulsions are produced during catastrophic phase inversion. These gel emulsions have the potential to diversify the applications in crude oil extraction, drug delivery systems, packaging materials, and other fields.

1. INTRODUCTION

Emulsion phase inversion is applied in a wide range of industries such as crude oil extraction, cosmetics, and pharmaceuticals.[1−5] Emulsion phase inversion is a phenomenon, in which the change of physicochemical properties results in different emulsion morphology (i.e., disperse phase is transformed into continuous phase and vice versa).[6−8] The emulsion microstructure near the phase inversion is important for predicting the postinversion emulsion microstructure and getting insight into the mechanism of emulsion phase inversion.[9−15] Hence, understanding the physicochemical properties of emulsions during phase inversion in depth can provide insightful references for emulsion applications and an understanding of the phase inversion mechanism.

The catastrophic phase inversion of emulsions is a process originating from the change in the volume ratio of oil to water.[10,11,16] Once the threshold value of the dispersed phase volume fraction is exceeded, a catastrophic phase inversion occurs.[17] Most of the results showed that the size and number of emulsion droplets increase with an increased volume fraction of the dispersed phase during catastrophic phase inversion. This forces an imbalance between coalescence and breakup of emulsion droplets, resulting in the transformation of the dispersed phase into a new continuous phase.[18,19] Based on this process, the qualitative characteristics including bimodality, sudden jumps, divergence, and hysteresis of the supposed cusp catastrophe theory were discovered by Thom.[20] Hysteresis means that the actual phase inversion line of the emulsion appears after the standard phase inversion line.[21] In other words, the internal phase volume fraction required for emulsion phase conversion is quite high. When the internal phase volume fraction is greater than 74%, the emulsion is a gel emulsion with high viscosity.[22]

To date, a large number of studies indicate that gel emulsions are formed during catastrophic phase inversion. For instance, Rondón-González et al.[11] investigated the effect of formulation, composition, and mixing conditions on the catastrophe phase inversion behavior of the transition from water-in-oil-in-water (W/O/W) to water-in-oil (W/O) emulsions. The results showed that gel emulsions with an

Received: August 22, 2022
Accepted: November 15, 2022
Published: November 27, 2022

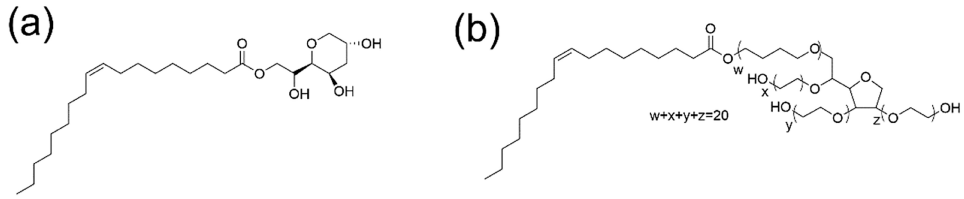

Figure 1. Molecular formulas of (a) Span 80 and (b) Tween 80.

internal phase volume fraction of 85% were formed near the phase inversion point. If enough energy is supplied to the emulsion, the curvature is forced to be approximately equal to zero. No gel emulsion was formed during the phase inversion process. If not, additional mixing time was needed to achieve the inversion process and form gel emulsions. Dunstan et al.[23] studied the catastrophic phase inversion from O/W to W/O emulsions, where W/O gel emulsions were formed at a lower oil volume fraction (φ_o). They found that catastrophic phase inversion of emulsion is related to not only HLB of the surfactant but also the contact angle. Liu et al.[1] studied the catastrophic phase inversion process from W/O to O/W emulsions. They confirmed that the inversion emulsion was not affected by the aqueous phase properties and always forms gel emulsions with viscoelasticity. However, the physicochemical properties of gel emulsions during catastrophic phase inversion are closely related to their structural and rheological properties, which have not been studied in depth.

Herein, the catastrophic phase inversion behavior was investigated by adjusting the HLB value and the aqueous phase properties of the surfactants. It is found that emulsions without NaCl formed O/W gel emulsions prior to phase inversion. The structure of the gel emulsion was studied macroscopically and microscopically at different φ_o. In particular, the rheological properties of the gel emulsions were studied and discussed in depth. The formation of gel emulsions provides new ways for their high-value utilization in crude oil extraction and gathering process and a deeper understanding of the emulsion catastrophic phase inversion mechanism.

2. EXPERIMENTAL SECTION

2.1. Chemicals and Materials. The oil phase was heptane (purity >99%, d = 0.684 g/cm^3, AR Sinopharm Chemical Reagent Co., Ltd.). The water phase was deionized water. The nonionic surfactants were lipophilic Sorbitan monooleate (Span 80, HLB = 4.3, AR, Sinopharm Chemical Reagent Co., Ltd.) and hydrophilic polyoxyethylene sorbitan monooleate (Tween 80, HLB = 15.0, AR, Sinopharm Chemical Reagent Co., Ltd.). All purchased reagents were used, without further purification. The chemical structures of Tween 80 and Span 80 surfactants are shown in Figure 1.

Surfactant concentration is represented by the weight volume fraction (w/v). The water/oil volume fraction is expressed as 100 vol % percent of the water/oil volume in emulsions (v/v).

2.2. Preparation of Emulsion. Initially, a quantity of surfactant (Span 80 and Tween 80) was dissolved in the deionized water. The oil phase was then added to the deionized water mixture containing the surfactants. The premeasured mixture was put into a jacketed beaker connected to the circulating water bath. The solution was kept at 40 °C for 10 min before stirring. Emulsions were prepared using a thermostatic method (40 °C) with high-speed emulsification using a homogenizer (Polytron PT 2500 E, Kinematica AG, Switzerland) at a speed of 10 000 r/min for 20 min. The homogenization process kept the rotating head of the disperser near the oil/water interface. For the emulsion preparation, the surfactant (Span 80 and Tween 80) concentrations were 2% (w/v).

2.3. Characterization of Materials. *2.3.1. Conductivity Measurements.* The conductivity of emulsions was tested within 30 s of the finish of emulsion preparation using an E4980AL precision LCR meter (Keysight Technologies Co., Ltd.) and Pt/Pt electrodes. High conductivity values represent O/W emulsions, while a low conductivity value represents W/O emulsions.

2.3.2. FTIR Spectroscopic Measurements. The inversion was detected by Fourier transform infrared spectroscopy (FTIR) using a Tensor II spectrometer (Germany Brooke Fourier Infrared Spectrometer Co., Ltd.). One microliter of emulsion was pipetted onto the center of a ZnSe window slice, and the IR spectrum of the emulsion sample was measured. The test conditions were as follows: detector DTGS, a spectral scan range of 4000−500 cm^{-1}, a scan time of 32 times, and a resolution of 2 cm^{-1}. FTIR of the emulsion formed under different conditions was recorded while measuring the conductivity of the emulsion.

2.3.3. Light Microscopy Imaging. The emulsion morphology was viewed using a BA310-T binocular projection polarized light microscope (Motic China Group Co., Ltd.) at a magnification of 400×. For prepared emulsions, 1 μL of the emulsion was pipetted onto a microscope slide. The emulsion was covered with a coverslip and pressed with microscope wipes to make the emulsion thinner.

2.3.4. Droplet Size Measurements. The average droplet size of emulsions was determined by dynamic light scattering (DLS) using a particle size analyzer (Brookhaven Instruments Corporation). All emulsions were diluted in continuous phase (water/heptane) to a proportion of 1:200 during particle size analysis. The average droplet size was analyzed with the instrument's analysis software (CONTIN mode).

2.3.5. Rheology Measurements. The rheology of the emulsions was tested using an Anton Paar MCR 302 rheometer (Thermo Fisher Scientific Co., Ltd.), which was operated by Rheoplus software. The temperature was kept at 25 °C during the measurement. The emulsion was placed in a concentric cylinder (CC27) and held for 5 min as the emulsion structure was restored. The conditions were as follows: (a) increased shear rate up to 100 s^{-1} from 1 s^{-1} and the emulsion viscosity/shear stress versus shear rate curve tested in flow mode; (b) increased strain up to 100% from 0.01% at a fixed angular frequency of 10 rad/s and viscoelastic properties of emulsion parameters, e.g., energy storage modulus (G') and loss modulus (G'').

https://doi.org/10.1021/acsomega.2c05388
ACS Omega 2022, 7, 44012−44020

2.3.6. Long-Term Stability Measurements. The prepared emulsions were added into cylindrical glass test tubes and analyzed for long-term stability using a Turbiscan Lab stability analyzer (Formulaction, L Union, France Co., Ltd.). The sensors were scanned upward along with the emulsion chamber from the bottom of the emulsion, acquiring transmitted and backscattered (BS) light data at a height of 55 μm. Measurements were taken at 5 min intervals at 50 °C for 3 h. The light intensity in the middle part of the backscattering point formed after the emulsion sample allows for the study of changes in stability at different times and locations within the emulsion system. The global stability of the emulsion was determined by the Turbiscan stability index (TSI).

3. RESULTS AND DISCUSSION

3.1. Monitoring of Emulsion Phase Inversion. When the surfactants used in the emulsions are mixed nonionic surfactants, the HLB value of the mixture is considered as the algebraic average of HLB values of single surfactants.

$$HLB_{mix} = HLB_A \times A\% + HLB_B \times B \quad (1)$$

where HLB_{mix} represents the HLB value of the mixed Span 80 and Tween 80, $HLB_{A/B}$ represents the HLB value of the surfactants Span 80 and Tween 80, and A% and B% represent the weight percentages of Span 80 and Tween 80, respectively.

The relationship between conductivity of emulsions stabilized by surfactants with different HLB values and φ_o

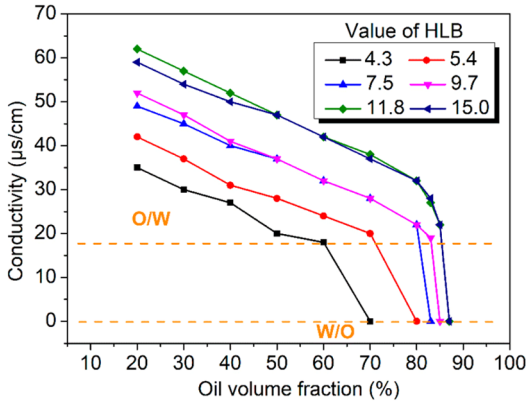

Figure 2. Conductivities versus oil volume fractions of the emulsions with different HLB values. The dotted line corresponds with the phase inversion.

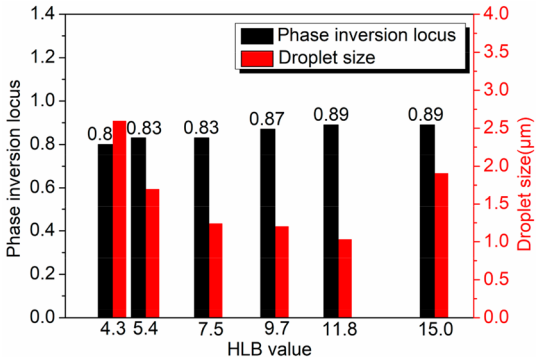

Figure 4. Droplet diameter (φ_o = 50%) and phase inversion locus of the emulsions versus HLB values.

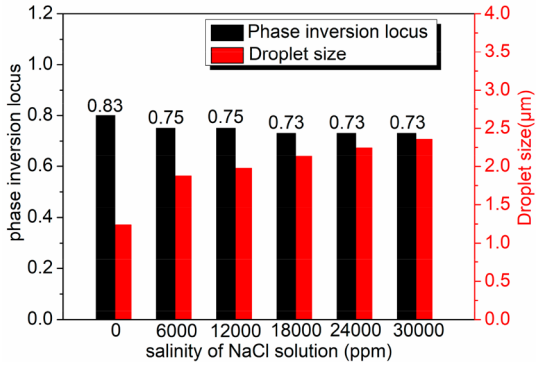

Figure 5. Droplet diameter (φ_o = 50%) and phase inversion locus of the emulsions versus the salinity of NaCl solution (HLB = 7.5).

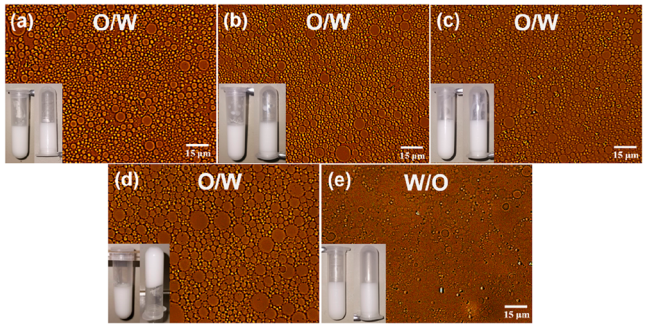

Figure 6. Micrographs of the emulsions (HLB = 7.5) with different oil volume fractions (400×): (a) 50%, (b) 60%, (c) 70%, (d) 80%, and (e) 83%. Bar equals 15 μm. The inset shows a typical picture of the physical appearance of gel emulsions at 25 °C.

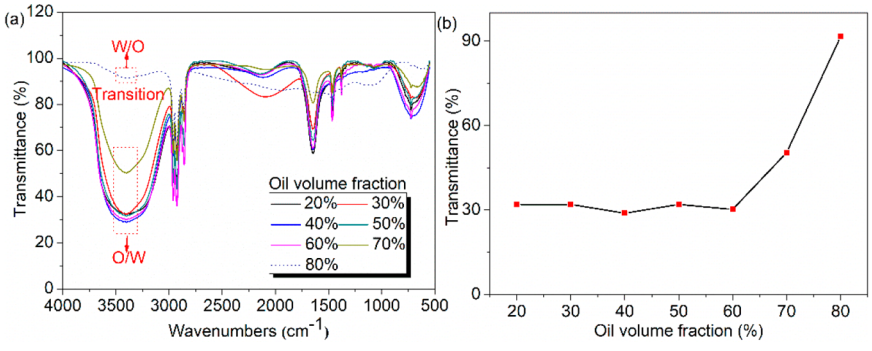

Figure 3. (a) FTIR spectra of the emulsions (HLB = 4.3) and (b) transmittances versus oil volume fractions (HLB = 4.3).

https://doi.org/10.1021/acsomega.2c05388
ACS Omega 2022, 7, 44012−44020

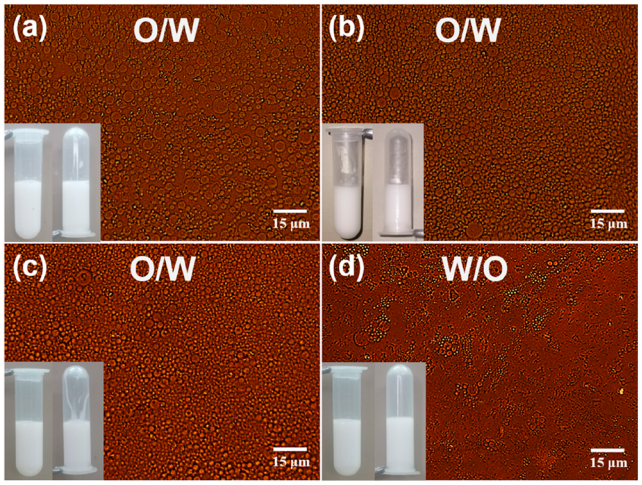

Figure 7. Micrographs of the emulsions (the salinity of NaCl solution = 12 000 ppm and HLB = 7.5) with different oil volume fractions (400×): (a) 60%, (b) 70%, (c) 73%, and (d) 75%. Bar equals 15 μm. The inset shows a typical picture of the physical appearance of gel emulsions at 25 °C.

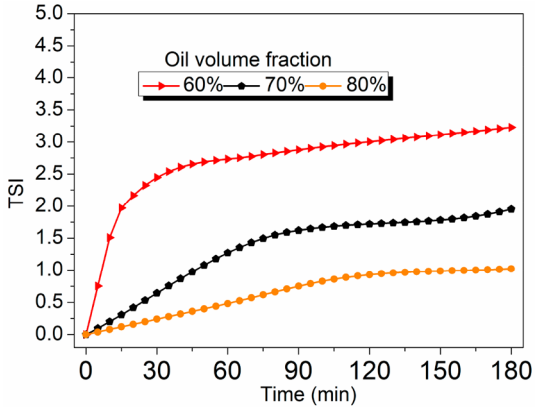

Figure 8. Stability (Turbiscan stability index values, TSI) of O/W emulsions versus oil volume fractions (HLB = 7.5).

was measured, as shown in Figure 2. As the increase of φ_o, the conductivity drastically decreases. As for these emulsions, the initial conductivity is very high (>35 μs/cm). However, it abruptly decreases to quite low values (~0.005 μs/cm) at the φ_o of 80−89%, indicating that the phase inversion appears. In addition, the conductivity tends to increase with increasing HLB value. This is because the adsorption of the nonionic surfactant with higher HLB value at the interface is stronger, which results in the increase of interface mobility.[24] As the conductivity difference is especially large among O/W and W/O emulsions, conductivity measurements can be used to differentiate emulsion types.

To compare the difference among the emulsion samples, the phase inversion was further determined by FTIR. As shown in Figure 3a and Figure S1, the peaks at 3200−3800 cm^{-1} are attributed to the stretching vibration of hydroxyl groups in water, Span 80, and Tween 80.[25,26] The peaks at 1630−1640 cm^{-1} are attributed to the bending vibration of hydroxyl groups in water.[27,28] There are significant differences in the FTIR spectra of emulsions before and after phase inversion. The significant weakening of the hydroxyl absorption peak of H_2O molecules results from the phase inversion from O/W to W/O emulsions. Based on FTIR results, the transmittance of the peak at 3400 cm^{-1} versus φ_o is shown in Figure 3b. When φ_o is less than 70%, the transmittance is around 30%. However, the transmittance abruptly increases to 91% at a φ_o of 80%, indicating the inversion occurred. The clear jump between the two O/W and W/O emulsions is consistent with the results of the phase inversion by conductivity measurements.

Figure 4 shows droplet diameter of emulsions and phase inversion locus versus HLB values of surfactants. The droplet diameter was determined by DLS. Emulsions that are made from either Span 80 or Tween 80 surfactants alone have a large droplet diameter. When the emulsion is made from mixed surfactants of Span 80 and Tween 80, its particle size is small. Generally, the smaller the droplet size in an emulsion, the more stable the emulsion. This indicates that mixed surfactants are more conducive to the stabilization of emulsions. Moreover, both the FTIR and conductivities results confirm that the phase inversion locus increases with the increase of HLB value. Based on the concept of interfacial spontaneous curvature on surfactant HLB values,[29] the best continuous phase for emulsions is the continuous phase with excellent surfactant solubility. The higher the hydrophilic Tween 80 content, the stronger the hydration interaction between the Tween 80 molecule and the water. This results in the increase of the occupied area of the Tween 80 headgroup. Thus, the assembly of Tween 80 molecules into the water is inhibited, leading to the interface easily bending into the convex shape toward the aqueous phase for accommodating the bulky headgroup.[30] As a result, emulsions have a relatively high phase inversion locus at higher HLB and a relatively low phase inversion locus at lower HLB values. Interestingly, the O/W gel emulsions are formed before the emulsion phase inversion at almost any HLB values, while the generation of O/W gel emulsions was only found at a few HLB values for the emulsion with the same surfactant.[12,31,32] This indicates that the regulation of HLB values of a mixed surfactant is vital to the performance of O/W gel emulsions.

To explore the effect of the salinity of NaCl solution on the phase inversion locus and droplet diameter of the emulsions, NaCl was added to the emulsion (Figure 5). The droplet diameter was determined by DLS. The phase inversion locus was determined by conductivity and FTIR (Figure S2 and Figure S3). The droplet diameter of emulsion in the absence of NaCl is smaller. In contrast, the presence of NaCl causes the increases in the emulsion droplet diameter. Furthermore, as the salinity of NaCl solution increases from 0 to 30000 ppm, the phase inversion locus tends to decrease. This is because the presence of Cl^- reduces the hydration of the polyoxyethylene chains in Tween 80 and the hydrogen bonding interactions of the hydroxyl groups in Span 80, leading to the reduction of hydrophilicity of the surfactant.[33] Na^+ also reduces the solubility of Tween 80 and Span 80 by dehydration and breaking hydrogen bonding interactions, respectively.[34,35] These two effects decrease the area occupied by the headgroup of the surfactant, which further decreases the spontaneous curvature of the surfactant on the oil/water interface. As the salinity of the NaCl solution increases, the area occupied by the headgroup of surfactant reduces to less than that occupied by the hydrophobic tailgroup. The spontaneous curvature of the surfactant layer is negative.[36,37] This indicates that the tendency of the spontaneous curvature of the surfactant layer toward the negative direction increases with the increase of the salinity of the NaCl solution. That means the emulsion phase

https://doi.org/10.1021/acsomega.2c05388
ACS Omega 2022, 7, 44012−44020

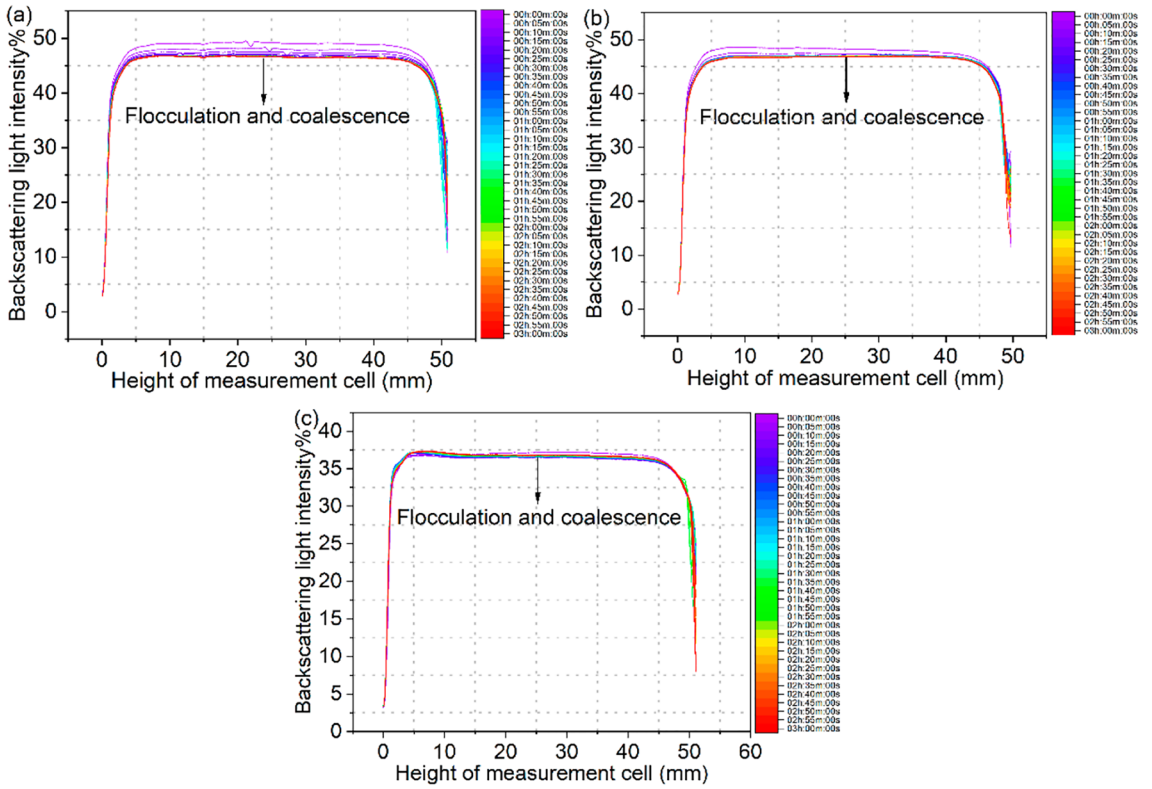

Figure 9. Backscattering curves of the O/W emulsions versus oil volume fractions (HLB = 7.5): (a) 60%, (b) 70%, and (c) 80%.

inversion locus decreases. Emulsions do not form gel emulsions when the φ_o is lower than 74%. Therefore, no gel emulsion is formed before the emulsion phase inversion with NaCl.

3.2. Morphology of Emulsion. In order to investigate the droplet structure of the emulsion near the phase inversion, the microscopic morphology of the emulsion was characterized by microscopy. The droplet morphology of the emulsions without NaCl at different φ_o values is shown in Figure 6. When φ_o is 80%, the O/W emulsion is a gel emulsion. The macrophotograph and microphotograph of the O/W gel emulsion is shown in Figure 6d. As can be observed from the digital photo, the gel emulsion is able to withstand its own gravity without flowing under inversion. From the microscope optical image, it can be observed that the gel emulsions show a polydisperse distribution. This is because the φ_o in the o/W gel emulsion is too high, causing the droplets in the emulsion to cluster closely to each other and form strong adhesions. This makes it difficult to form an emulsion with uniform droplet size.[38,39] The density of droplets of W/O emulsions, without NaCl, decreased significantly (Figure 6e). In the absence of NaCl, gel emulsion was formed during the catastrophic phase inversion.

When adding NaCl, φ_o increases from 60% to 75%, and the droplet diameter decreases slightly (Figure 7). The density of droplets of W/O emulsions, with NaCl, decreases significantly (Figure 7d). It can be observed from the digital photo that the emulsion is not able to withstand its own gravity and flows in an inverted situation. In the presence of NaCl, no gel emulsion is formed during the catastrophic phase inversion.

3.3. Stability of the O/W Gel Emulsion. As is well-known, gel emulsions do not have good stability at high temperatures. Therefore, the stability of gel emulsions at 50 °C was further determined. The dependence of global TSI values versus standing time of O/W emulsions with different φ_o at 50 °C is shown in Figure 8. It is known that lower TSI values correspond to higher emulsion stability.[40] When the φ_o is 60%, the TSI value dramatically increases with time in a short period (0−60 min). This indicates a relatively strong change in the internal state of the O/W emulsion during this period. When the system is O/W gel emulsion (φ_o = 80%), the TSI value increases slowly with time over a relatively short duration of time. Subsequently, the TSI values of all O/W emulsions tend to be stable, indicating that the emulsions reach a stable state at this time. It can be concluded that the TSI value is the smallest for the system of O/W gel emulsion at the same time. This indicates that the O/W gel emulsion before the phase inversion has good stability at 50 °C.

Figure 9 shows the backscattering curves for O/W emulsions with different φ_o values at 50 °C. The curve shows blue at 0 h and gradually changes to red at 3 h. The main manifestations of emulsion instability are flocculation and coalescence.[41] The curve of BS light intensity versus time in the emulsion sample can be used to reflect the degree of flocculation and coalescence of the emulsion. The more stable the emulsion, the smaller the variation in BS curve.[42] As shown in Figure 9c, the BS light intensities of the O/W gel emulsion sample with φ_o = 80% are similar at all times and each height, with the curves almost overlapping, indicating that the emulsions were the most stable. By contrast, a significant variation is observed for the BS light intensity with a φ_o of 60% (Figure 9a). In this case, the emulsion is more unstable. In addition, the backscattering of the bottom gel emulsion (φ_o = 80%) decreases more slowly with time compared to the other normal emulsions. This phenomenon is due to its higher viscosity, which hinders droplet migration.[43] The BS light curves of the O/W water/Span 80-Tween 80/heptane emulsions prior to

https://doi.org/10.1021/acsomega.2c05388
ACS Omega 2022, 7, 44012−44020

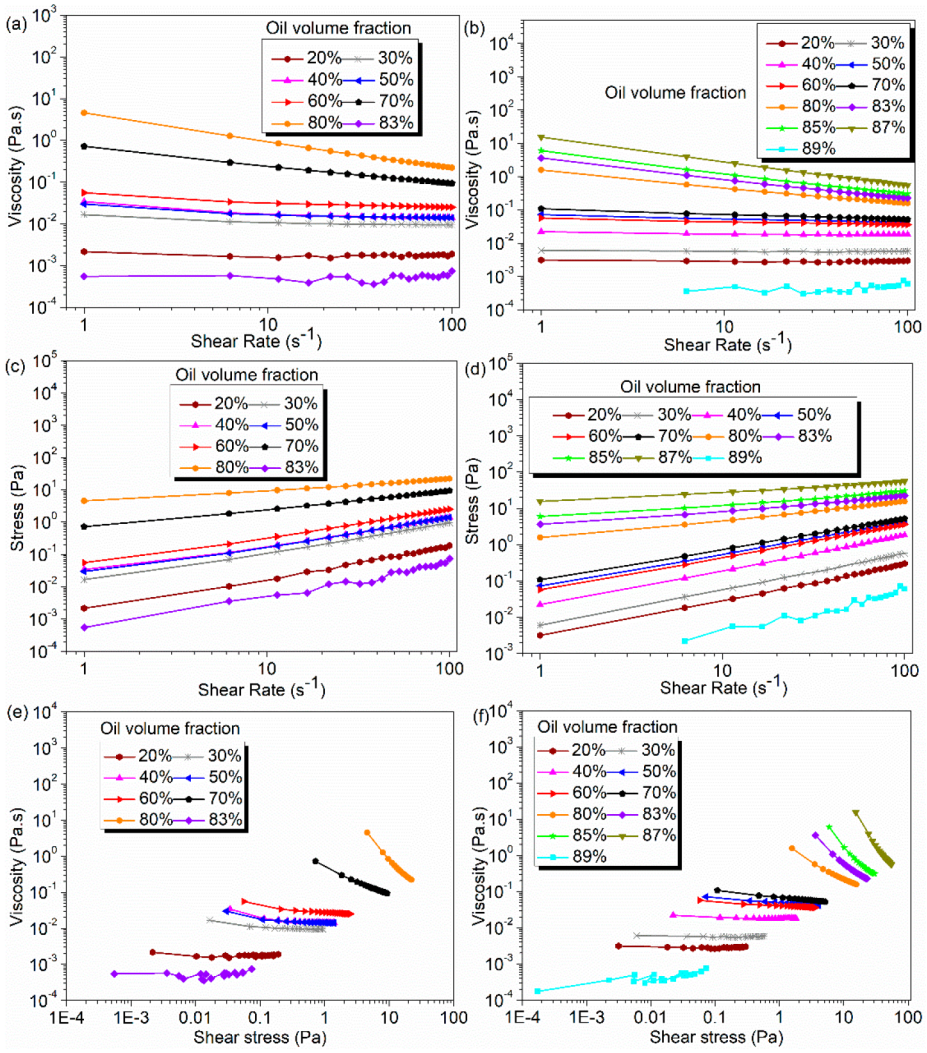

Figure 10. Shear viscosity versus shear rate of the emulsions with different HLB values: (a) HLB = 7.5, (b) HLB = 11.8. Shear stress versus shear rate of the emulsions with different HLB values: (c) HLB = 7.5, (d) HLB = 11.8. Shear viscosity versus shear stress of the emulsions with different HLB values: (e) HLB = 7.5, (f) HLB = 11.8.

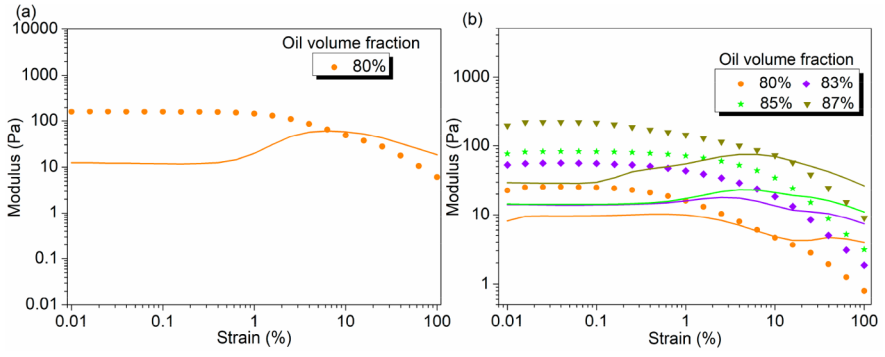

Figure 11. Storage modulus G' (symbols) and loss modulus G'' (lines) versus strain of the O/W gel emulsions with different HLB values: (a) HLB = 7.5 and (b) HLB = 11.8.

the phase inversion show that the O/W gel emulsion before the phase inversion has good stability at 50 °C.

3.4. Rheological Behavior of Gel-Emulsion at Phase Inversion. Rheological properties are one of the most important properties of emulsions, reflecting the stability and functionality of emulsions. For a deeper comprehension of the internal structure of gel emulsions, an investigation of the rheological properties of different φ_o emulsions during phase inversion was conducted.

Apparent viscosity/stress as a function of shear rate curves for emulsions was tested under the flow mode. As shown in Figure 10a–d and Figure S4a–d, the apparent viscosity

https://doi.org/10.1021/acsomega.2c05388
ACS Omega 2022, 7, 44012−44020

decreases and the shear stress increases as the shear rate increases from 1 s^{-1} to 100 s^{-1}. These emulsions exhibit typical shear-thinning flow behavior. All emulsions behaved as a non-Newtonian fluid. Prior to phase inversion of emulsions, the higher φ_o, the higher the apparent viscosity of O/W emulsion at the same shear rate. However, the emulsion recovers its liquidity when the inversion is complete, which is consistent with previous studies.[44] The results show that, at the same shear rate, the viscosity and shear stress values of the O/W gel emulsions are significantly higher than other normal emulsions prior to phase inversion.

The relationship between shear stress and apparent viscosity of the emulsions is given in Figure 10e,f and Figure S4e,f. The apparent viscosity of emulsions increases at low shear stress. According to this phenomenon, the existence of yield stress is proved.[45] The yield stress is used to characterize the structural stiffness and stability of emulsion. It describes the degree of deformation that emulsions can withstand without causing permanent structural damage.[46] The high yield stress can prevent the emulsion from separating between oil and water phases, precipitation or droplet aggregation.[47] The yield stress of the O/W gel emulsions is significantly higher than those of other normal emulsions prior to phase inversion. This means that O/W gel emulsions are more stable.

The yield strain of emulsions was tested using the amplitude scanning mode (Figure 11). The G' of the O/W gel emulsions is consistently greater than the G'' of the O/W gel emulsions as the strain increases to around 10%. This exhibits typical gel emulsion behavior.[48] At low shear strains, both G' and G'' of the O/W gel emulsions remain at a constant value with a significant linear viscoelastic (LVE) zone. As the shear strain further increases, G' begins to fall and G'' begins to rise, during which a critical strain (yield strain) appears. This transition suggests that the gel-like network structure of the emulsion is disrupted and begins to rearrange, which is in agreement with Mason's study.[49] Both G' and G'' increase together with an increase in φ_o. This indicates that the higher the φ_o, the stronger the gel strength of the emulsion and the more stable the emulsion. As for φ_o and emulsion rheology, the increase of φ_o leads to increasing G' and G''. Moreover, increasing φ_o facilitates the enhancement of the gel-like network structure of the gel emulsion. This contributed to the formation of a tightly packed structure, thus improving the stability of the emulsion.[50] The rheological results show that the viscosity, shear stress, and elastic modulus of gel emulsions increase significantly as φ_o increase before the catastrophic phase inversion.

4. CONCLUSIONS

The influence of the HLB value of a nonionic surfactant (Span 80 and Tween 80) and aqueous phase properties (with or without NaCl in emulsions) on the catastrophic phase inversion of O/W model emulsion was investigated. In the absence of NaCl in emulsions, the phase inversion locus increases with increasing surfactant HLB value. The emulsions with Span 80 or Tween 80 surfactants alone have larger particle sizes. The particle size of the emulsions is smaller when emulsions are made from mixed surfactants of Span 80 and Tween 80. O/W gel emulsions, without NaCl, are formed prior to phase inversion. In terms of rheological properties, the emulsion close to the phase inversion exhibits typical gel emulsion behavior. At the same shear rate, the viscosity, shear stress, and modulus of elasticity of gel emulsions increase significantly with the increase of φ_o before phase inversion. The Turbiscan Lab stability analyzer indicates that O/W gel emulsions before the phase inversion has good stability at 50 °C. When the emulsion contains NaCl, as the salinity of NaCl increases, the phase inversion locus decreases and the emulsion droplet diameter increases. O/W gel emulsions are not formed prior to phase inversion. Therefore, the behavior of emulsion phase inversion is regulated via changing physicochemical properties of emulsions. The formation of gel emulsion provides references for research in the fields of crude oil extraction, drug delivery systems, and packaging materials.

■ ASSOCIATED CONTENT

Supporting Information

The Supporting Information is available free of charge at https://pubs.acs.org/doi/10.1021/acsomega.2c05388.

FTIR spectra of emulsions with HLB = 7.5, HLB = 9.7, and HLB = 11.8 versus oil volume fractions; conductivities versus oil volume fractions of the emulsions with the salinity of NaCl solution; FTIR spectra of the emulsions with the salinity of NaCl solution (12 000 and 18 000 ppm) versus oil volume fractions; steady shear viscosity as a function of shear rate of the emulsions with HLB = 4.3 and HLB = 9.7; steady shear stress as a function of shear rate of the emulsions with HLB = 4.3 and HLB = 9.7 and steady shear viscosity as a function of shear stress of the emulsions with HLB = 4.3 and HLB = 9.7 (PDF)

■ AUTHOR INFORMATION

Corresponding Author

Longli Zhang − *College of Chemistry and Chemical Engineering, China University of Petroleum (East China), Qingdao 266580, China;* orcid.org/0000-0001-8546-387X; Phone: +86 532 86983374; Email: llzhang@upc.edu.cn; Fax: +86 532 86983369

Authors

Jie Jiang − *College of Chemistry and Chemical Engineering, China University of Petroleum (East China), Qingdao 266580, China*

Zi Wang − *College of Chemistry and Chemical Engineering, China University of Petroleum (East China), Qingdao 266580, China*

Chuangye Wang − *College of Chemistry and Chemical Engineering, China University of Petroleum (East China), Qingdao 266580, China*

Lina Shi − *College of Science, China University of Petroleum (East China), Qingdao 266580, China*

Jian Hou − *School of Petroleum Engineering, China University of Petroleum (East China), Qingdao 266580, China*

Complete contact information is available at: https://pubs.acs.org/10.1021/acsomega.2c05388

Notes

The authors declare no competing financial interest.

■ ACKNOWLEDGMENTS

The authors greatly appreciate the financial support of the National Key Research and Development Program of China (Grant No. 2018YFA0702400), the National Natural Science

Foundation of China (Grant No. 21576292), and the Natural Science Foundation of Shandong Province (ZR2020ME088).

REFERENCES

(1) Liu, Y.; Carter, E. L.; Gordon, G. V.; Feng, Q. J.; Friberg, S. E. An investigation into the relationship between catastrophic inversion and emulsion phase behaviors. *Colloids Surf. A: Physicochem. Eng. Asp.* **2012**, *399*, 25−34.
(2) Lee, J.; Babadagli, T. Comprehensive review on heavy-oil emulsions: Colloid science and practical applications. *Chem. Eng. Sci.* **2020**, *228*, 115962.
(3) de Oliveira Honse, S.; Kashefi, K.; Charin, R. M.; Tavares, F. W.; Pinto, J. C.; Nele, M. Emulsion phase inversion of model and crude oil systems detected by near-infrared spectroscopy and principal component analysis. *Colloids Surf. A: Physicochem. Eng. Asp.* **2018**, *538*, 565−573.
(4) Plasencia, J.; Pettersen, B.; Nydal, O. J. Pipe flow of water-in-crude oil emulsions: Effective viscosity, inversion point and droplet size distribution. *J. Petrol. Sci. Eng.* **2013**, *101*, 35−43.
(5) Azmi, N. A. N.; Elgharbawy, A. A.; Motlagh, S. R.; Samsudin, N.; Salleh, H. M. Nanoemulsions: Factory for food, pharmaceutical and cosmetics. *Processes* **2019**, *7*, 617.
(6) Cabaleiro, D.; Agresti, F.; Fedele, L.; Barison, S.; Hermida-Merino, C.; Losada-Barreiro, S.; Bobbo, S.; Piñeiro, M. M. Review on phase change material emulsions for advanced thermal management: Design, characterization and thermal performance. *Renew. Sust. Energy Rev.* **2022**, *159*, 112238.
(7) Mir, M.; Ghasemirad, S. Phase inversion emulsification of paraffin oil/polyethylene wax blend in water: A comparison between mixed monomeric and monomeric/gemini surfactant systems. *J. Mol. Liq.* **2022**, *359*, 119315.
(8) Mei, Z.; Xu, J.; Sun, D. O/W nano-emulsions with tunable PIT induced by inorganic salts. *Colloids Surf. A: Physicochem. Eng. Asp.* **2011**, *375*, 102−108.
(9) Ling, N. N.; Haber, A.; May, E. F.; Fridjonsson, E. O.; Johns, M. L. NMR studies of emulsion microstructure approaching the phase inversion point. *Colloids Surf. A: Physicochem. Eng. Asp.* **2014**, *462*, 244−251.
(10) Perazzo, A.; Preziosi, V.; Guido, S. Phase inversion emulsification: Current understanding and applications. *Adv. Colloid Interface Sci.* **2015**, *222*, 581−599.
(11) Rondón-González, M.; Sadtler, V.; Marchal, P.; Choplin, L.; Salager, J. L. Emulsion catastrophic inversion from abnormal to normal morphology. 7. Emulsion evolution produced by continuous stirring to generate a very high internal phase ratio emulsion. *Ind. Eng. Chem. Res.* **2008**, *47*, 2314−2319.
(12) Lv, G.; Wang, F.; Cai, W.; Zhang, X. Characterization of the emulsions formed by catastrophic phase inversion. *Colloids Surf. A: Physicochem. Eng. Asp.* **2014**, *450*, 141−147.
(13) Liu, W.; Sun, D.; Li, C.; Liu, Q.; Xu, J. Formation and stability of paraffin oil-in-water nano-emulsions prepared by the emulsion inversion point method. *J. Colloid Interface Sci.* **2006**, *303*, 557−563.
(14) Mir, M.; Ghasemirad, S. Phase inversion emulsification of paraffin oil/polyethylene wax blend in water: A comparison between mixed monomeric and monomeric/gemini surfactant systems. *J. Mol. Liq.* **2022**, *359*, 119315.
(15) Wang, X.; Lu, X.; Wen, L.; Yin, Z. Incomplete phase inversion W/O/W emulsion and formation mechanism from an interfacial perspective. *J. Disper. Sci. Technol.* **2018**, *39*, 122−129.
(16) Lv, G.; Wang, F.; Cai, W.; Zhang, X. Characterization of the addition of lipophilic Span 80 to the hydrophilic Tween 80-stabilized emulsions. *Colloids Surf. A: Physicochem. Eng. Asp.* **2014**, *447*, 8−13.
(17) Binks, B. P.; Lumsdon, S. O. Catastrophic inversion of water-in-oil emulsions stabilized by hydrophobic silica. *Langmuir* **2000**, *16*, 2539−2547.
(18) Maffi, J. M.; Meira, G. R.; Estenoz, D. A. Mechanisms and conditions that affect phase inversion processes. A review. *Can. J. Chem. Eng.* **2021**, *99*, 178−208.
(19) Tyrode, E.; Mira, I.; Zambrano, N.; Márquez, L.; Rondon-Gonzalez, M.; Salager, J. L. Emulsion catastrophic inversion from abnormal to normal morphology. 3. Conditions for triggering the dynamic inversion and application to industrial processes. *Ind. Eng. Chem. Res.* **2003**, *42*, 4311−4318.
(20) Thom, R. Stabilité structurelle et morphogenèse. *Poetics* **1974**, *3*, 7−19.
(21) Pierlot, C.; Ontiveros, J. F.; Royer, M.; Catte, M.; Salager, J. L. Emulsification of viscous alkyd resin by catastrophic phase inversion with nonionic surfactant. *Colloids Surf. A: Physicochem. Eng. Asp.* **2018**, *536*, 113−124.
(22) Lee, M. C.; Tan, C.; Ravanfar, R.; Abbaspourrad, A. Ultrastable water-in-oil high internal phase emulsions featuring interfacial and biphasic network stabilization. *ACS Appl. Mater. Interfaces* **2019**, *11*, 26433−26441.
(23) Dunstan, T. S.; Fletcher, P. D.; Mashinchi, S. High internal phase emulsions: Catastrophic phase inversion, stability, and triggered destabilization. *Langmuir* **2012**, *28*, 339−349.
(24) Bera, A.; Kumar, S.; Mandal, A. Temperature-dependent phase behavior, particle size, and conductivity of middle-phase microemulsions stabilized by ethoxylated nonionic surfactants. *J. Chem. Eng. Data* **2012**, *57*, 3617−3623.
(25) Bora, M. M.; Gogoi, P.; Deka, D. C.; Kakati, D. K. Synthesis and characterization of yellow oleander (Thevetia peruviana) seed oil-based alkyd resin. *Ind. Crop. Prod.* **2014**, *52*, 721−728.
(26) Gong, M.; Yang, J.; Zhang, J.; Zhu, H.; Tong, T. Physical−chemical properties of aged asphalt rejuvenated by bio-oil derived from biodiesel residue. *Constr. Build. Mater.* **2016**, *105*, 35−45.
(27) Bal'Zhinimaev, B. S.; Paukshtis, E. A.; Toktarev, A. V.; Kovalyov, E. V.; Yaranova, M. A.; Smirnov, A. E.; Stompel, S. Effect of water on toluene adsorption over high silica zeolites. *Micropor Mesopor Mater.* **2019**, *277*, 70−77.
(28) Heitmann, G. P.; Dahlhoff, G.; Niederer, J. P. M.; Hölderich, W. F. Active sites of a [B]-ZSM-5 Zeolite catalyst for the Beckmann rearrangement of cyclohexanone oxime to caprolactam. *J. Catal.* **2000**, *194*, 122−129.
(29) Bancroft, W. D. The theory of emulsification. *J. Phys. Chem.* **1913**, *17*, 501.
(30) Kumar, A.; Li, S.; Cheng, C. M.; Lee, D. Recent developments in phase inversion emulsification. *Ind. Eng. Chem. Res.* **2015**, *54*, 8375−8396.
(31) Preetika, R.; Mehta, P. S.; Kaisare, N. S.; Basavaraj, M. G. Kinetic stability of surfactant stabilized water-in-diesel emulsion fuels. *Fuel* **2019**, *236*, 1415−1422.
(32) Esposito, R.; Cavasso, D.; Niccoli, M.; D'Errico, G. Phase Inversion and Interfacial Layer Microstructure in Emulsions Stabilized by Glycosurfactant Mixtures. *Nanomaterials* **2021**, *11*, 331.
(33) Anton, N.; Saulnier, P.; Beduneau, A.; Benoit, J. P. Salting-out effect induced by temperature cycling on a water/nonionic surfactant/oil system. *J. Phys. Chem. B* **2007**, *111*, 3651−3657.
(34) Schott, H.; Han, S. K. Effect of inorganic additives on solutions of nonionic surfactants II. *J. Pharm. Sci.* **1975**, *64*, 658−664.
(35) Schott, H. Effect of inorganic additives on solutions of nonionic surfactants: X. micellar properties. *J. Colloid Interface Sci.* **1995**, *173*, 265−277.
(36) Chen, W.; Schechter, D. S. Surfactant selection for enhanced oil recovery based on surfactant molecular structure in unconventional liquid reservoirs. *J. Petrol. Sci. Eng.* **2021**, *196*, 107702.
(37) Mei, Z.; Xu, J.; Sun, D. O/W nano-emulsions with tunable PIT induced by inorganic salts. *Colloids Surf. A: Physicochem. Eng. Asp.* **2011**, *375*, 102−108.
(38) Tong, Q.; Yi, Z.; Ran, Y.; Chen, X.; Chen, G.; Li, X. Green tea polyphenol-stabilized gel-like high internal phase pickering emulsions. *ACS Sustain. Chem. Eng.* **2021**, *9*, 4076−4090.
(39) Bibette, J.; Mason, T. G.; Hu, G.; Weitz, D. A. Kinetically Induced Ordering in Gelation of Emulsions. *Phys. Rev. Lett.* **1992**, *69*, 981−984.
(40) Ji, Y.; Kang, W.; Meng, L.; Hu, L.; Yang, H. Study of the solution behavior of β-cyclodextrin amphiphilic polymer inclusion

https://doi.org/10.1021/acsomega.2c05388
ACS Omega 2022, 7, 44012−44020

complex and the stability of its O/W emulsion. *Colloids Surf. A: Physicochem. Eng. Asp.* **2014**, *453*, 117−124.
(41) García-Tejeda, Y. V.; Leal-Castañeda, E. J.; Espinosa-Solis, V.; Barrera-Figueroa, V. Synthesis and characterization of rice starch laurate as food-grade emulsifier for canola oil-in-water emulsions. *Carbohydr. Polym.* **2018**, *194*, 177−183.
(42) Felix, M.; Romero, A.; Guerrero, A. Influence of pH and Xanthan Gum on long-term stability of crayfish-based emulsions. *Food Hydrocolloids* **2017**, *72*, 372−380.
(43) Huang, K.; Liu, R.; Zhang, Y.; Guan, X. Characteristics of two cedarwood essential oil emulsions and their antioxidant and antibacterial activities. *Food Chem.* **2021**, *346*, 128970.
(44) Zhao, Z.; Liu, W.; Liu, Z.; Ding, P.; Li, H. Phase inversion of TiO_2 nanoparticle stabilized emulsions of alkenyl succinic anhydride. *Chem. Eng. Sci.* **2013**, *87*, 246−257.
(45) Pajouhandeh, A.; Kavousi, A.; Schaffie, M.; Ranjbar, M. Experimental measurement and modeling of nanoparticle-stabilized emulsion rheological behavior. *Colloids Surf. A: Physicochem. Eng. Asp.* **2017**, *520*, 597−611.
(46) Shahbazi, M.; Jäger, H.; Ettelaie, R. Application of Pickering emulsions in 3D printing of personalized nutrition. Part I: Development of reduced-fat printable casein-based ink. *Colloids Surf. A: Physicochem. Eng. Asp.* **2021**, *622*, 126641.
(47) Kim, H. S.; Mason, T. G. Advances and challenges in the rheology of concentrated emulsions and nanoemulsions. *Adv. Colloid Interface Sci.* **2017**, *247*, 397−412.
(48) Yousefi, A. R.; Razavi, S. M. Dynamic rheological properties of wheat starch gels as affected by chemical modification and concentration. *Starch-Starke* **2015**, *67*, 567−576.
(49) Mason, T. G.; Bibette, J.; Weitz, D. A. Elasticity of Compressed Emulsions. *Phys. Rev. Lett.* **1995**, *75*, 2051−2054.
(50) Shao, Y.; Tang, C. H. Gel-like pea protein Pickering emulsions at pH 3.0 as a potential intestine-targeted and sustained-release delivery system for *β*-carotene. *Food Res. Int.* **2016**, *79*, 64−72.

https://doi.org/10.1021/acsomega.2c05388
ACS Omega 2022, 7, 44012−44020